State Space Modeling and Feedback Control of Five-phase Permanent Magnet Assisted Synchronous Reluctance Motor under Open Phase Faults

AKM Arafat and Seungdeog Choi
Department of Electrical & Computer Engineering
The University of Akron
Akron, OH, USA

***Abstract*—This paper presents an analysis of the state space modeling (SSM) and feedback control method of a five-phase permanent magnet assisted synchronous reluctance motor (PMa-SynRM) under open phase faults. Primarily, the reliability of an electrical machine is of prime concern for the safety-critical applications. Therefore, the innovative and reliable control methods are required to derive better fault tolerant operation of a five-phase PMa-SynRM successfully. Classical control methods have been widely accepted to control the electric machines. However, modern control technique is better suited for controlling any multi-input and multi-output (MIMO) system, for example, direct and quadratic axis control of the electric machine. However, the performance of the modern control method has been limitedly studied under different open phase fault conditions in PMa-SynRM. This paper develops a modern control technique which utilizes a state space equivalent model (SSEM) of the PMa-SynRM under different open phase faults. The SSEM is used to develop the state feedback control method. For further analyzing stability criterion a Lyapunov function is used along with detail explanation of the proposed theory. The stability analysis are carried out through extensive MATLAB simulation.**

***Index Terms*—Permanent magnet motors, Motor drives, State space modeling, State feedback control**

NOMENCLATURE

d, q axis	Synchronously rotating direct and quadrature axes
T_{xform}	Transformation matrix for transforming parameters from $ABCDE$ to $d-q$ axis components
V_d, V_q	Voltages in the $d-q$ axis
I_d, I_q	Currents in the $d-q$ axis
R_{abcde}	Phase resistances in $ABCDE$ phases
T_e	Electromagnetic torque
$R_{\alpha 1 \beta 1 \alpha 3 \beta 3)}$	Resistances in the stationary reference frame ($\alpha-\beta$ axis)
$R_{d1q1d3q30)}$	Resistances in the $d-q$ axis
R_{d1}, R_{q1}	Resistances for the fundamental
R_{d3}, R_{q3}	Resistances for the third harmonic
R_0	Zero sequence resistance
$H(s)_{dq,OL}$	s-domain open loop transfer function in $d-q$ axis
$H(s)_{dq,CL}$	s-domain closed loop transfer function in $d-q$ axis
A_x, B_x, C_x	Original system matrices
$\zeta_{SPF}, \zeta_{TPAF}$	Desired pole location of the system under single phase open and two-phase adjacent open fault conditions
$\tilde{A_x}, \tilde{B_x}, \tilde{C_x}$	Modified system matrices considering state feedback
$\tilde{k}_{SPF}, \tilde{k}_{TPAF}$	state feedback gains under single phase open and two-phase adjacent open fault conditions

I. INTRODUCTION

The popularity of five-phase electrical machines for reliable applications has been mounting in recent years due to their additional advantages over the conventional three-phase machines [1], [2]. The major advantages include high power density, reduced torque ripple, and higher fault tolerance capability [3], [4]. Several control methods have been proposed to enhance the fault tolerant operation of the five-phase permanent motor under various open phase faults [5]–[7]. Most of the control methods have followed the traditional control (fundamentally PID controller) approach to provide better dynamic performances under fault-tolerant operation. These control techniques are widely granted in industries due to their simplicity and easier implementation. However, the PID controller requires frequent parameter tuning which becomes challenging under critical fault conditions in F-PMa-SynRM. In other ways, modern control method such as state feedback control has been applied in many non-linear systems where the system dynamics require better stability characteristics. However, this control method has been limitedly reported in earlier studies for electric motor drives. Therefore, the further investigation of the state feedback controller is necessary to provide optimal fault tolerant operation under various open phase faults.

Classical control theory has been popular for analyzing any SISO (single input, single output) systems [8], [9]. This control technique has also been applied in electric motor drives [10],

978-1-5386-1180-7/18/$31.00 ©2018 IEEE

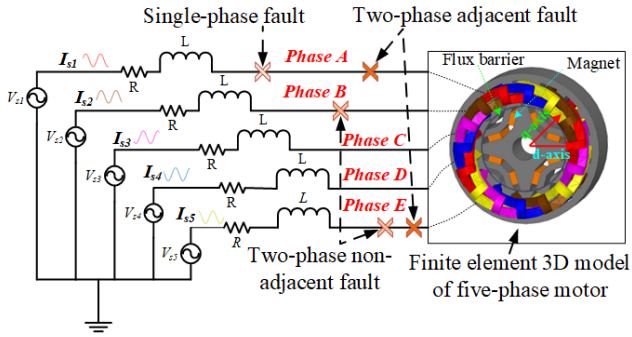

Fig. 1: Different unbalanced resistance condition in five-phase

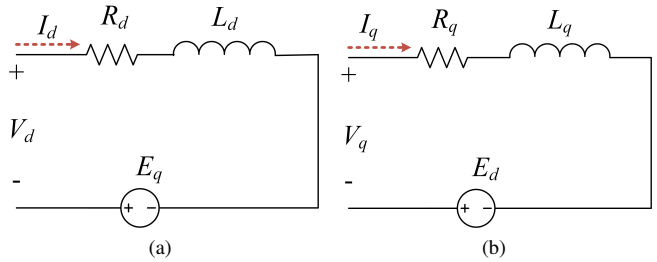

Fig. 2: $d-q$ axis equivalent circuit model: (a) d-axis and (b) q-axis.

[11]. However, a state space feedback control approach is better suited for any MIMO (multi-input and multi-output) systems [12], [13]. Fundamentally, electric motor drives employ the DQ axes current control methods which resemble a MIMO system with multi-variable. The state feedback control method can handle the non-linearity and the time-invariant characteristics of a real MIMO system suitably.

Research are conducted on state feedback control for electric motor drives. State space vector model of a linear induction motor has been discussed in [14]. For a self-excited induction generator, a linearized state space model has been developed in [15]. Model prediction based state space control has been studied in [16]. A stable load-torque model-reference-adaptive-system (MRAS) estimator has also been developed in [17]. However, under open phase faults in F-PMa-SynRM, the modeling and performance analysis of a state feedback control algorithm has been limitedly studied.

In this paper, the nonlinear equivalent mathematical model of the F-PMa-SynRM under open phase fault has been linearized (SSEM). Utilizing the SSEM, the analytical values of the state feedback gains are computed. The SSEM and the state feedback gains are used for serving better dynamic performances under the fault-tolerant operation of F-PMa-SynRM. Detail The theoretical analysis is validated through extensive MATLAB simulation.

II. MATHEMATICAL MODELING OF THE FIVE-PHASE SYSTEM UNDER FAULTS

To study state feedback control under different open phase faults, the five-phase PMa-SynRM drive has been modeled showing possible open phase faults in Fig. 1. It shows various open phase faults including the SPF (Phase A = 0), TPAF (phases AE = 0), and TPNF (phases BE = 0) open faults. In this paper, detail analysis under healthy, SPF, and TPAF conditions are done.

The five-phase currents can be represented as follows:

$$I_{s\lambda} = I_{\lambda}\sin(2\pi ft - \alpha 2\pi/5) \tag{1}$$

where, $I_{s\lambda}$ is the healthy phase currents, I_{λ} is the magnitudes of the phase current, λ is the phase number, and α is the integer as $0-4$ based on phase number. The phase resistances can be presented as follows:

$$[R_{abcde}] = \begin{bmatrix} R_a & 0 & 0 & 0 & 0 \\ 0 & R_b & 0 & 0 & 0 \\ 0 & 0 & R_c & 0 & 0 \\ 0 & 0 & 0 & R_d & 0 \\ 0 & 0 & 0 & 0 & R_e \end{bmatrix} \tag{2}$$

Conventionally, a synchronous machine is mathematically represented and analyzed in synchronously rotating frame known as $d-q$ axes. Following that, the most of the control methods are also developed in this rotating reference frame. For this reason, the phase parameters need to transform to this $d-q$ reference frame. The transformation matrix is derived as below:

$$[T_{xform}] = \frac{2}{5}\begin{bmatrix} 1 & \cos\mu & \cos 2\mu & \cos 3\mu & \cos 2\mu \\ 0 & \sin\mu & \sin 2\mu & \sin 3\mu & \sin 4\mu \\ 1 & \cos 3\mu & \cos 6\mu & \cos 9\mu & \cos 12\mu \\ 0 & \sin 3\mu & \sin 6\mu & \sin 9\mu & \sin 12\mu \\ \frac{1}{2} & \frac{1}{2} & \frac{1}{2} & \frac{1}{2} & \frac{1}{2} \end{bmatrix} \tag{3}$$

where, $\mu = 2\pi/5$. Using this transformation matrix, the phase parameters of Fig. 1 can be transformed to the $d-q$ axes phase parameters. In (3), the first two rows are the contribution from the fundamental signals in the $d-q$ axis frame. Second two rows are the contribution from third harmonics in the $d-q$ axis frame. In this paper, the fundamental signal is considered during the modeling and control. The $d-q$ axes equivalent models are shown in the Fig. 2. From this Fig. 2, the equivalent dynamic model in the $d-q$ reference frame can be derived as follows:

$$
\begin{aligned}
V_d &= R_a I_d + L_d \frac{dI_d}{dt} + E_q \\
V_q &= R_a I_q + L_q \frac{dI_q}{dt} + E_d \\
E_d &= -\omega_r (L_q(I_q) - \lambda_{PM}) \\
E_q &= \omega_r L_d I_d
\end{aligned} \tag{4}
$$

where, R_a is the winding resistance, V_d and I_d are d-axis and V_q and I_q are the q-axis average voltage and current, L_d is the d-axis inductance, L_q is the q-axis inductance, λ_{PM} is the permanent magnet flux linkage, and E_q and E_d are the back electromotive forces in the d-axis and q-axis, respectively. The output torque equation can be derived as follows:

$$
T_e = K(\lambda_{PM} I_d + (L_d - L_q) I_d I_q) \tag{5}
$$

where K is $\frac{5P}{4}$. In (5).

It is expected, the phase parameters become different under open phase faults. As the phase resistances has a significant contribution to real power generation, the equivalent model has to be re-defined under fault conditions. The transformation of the phase resistances to the stationary reference axis can be done as follows:

$$
R_{\alpha 1 \beta 1 \alpha 3 \beta 30} = T_{xform} R_{abcde} T_{xform}^{-1} \tag{6}
$$

The phase resistances can be transformed to the rotating reference axis from the stationary reference axis. This transformation can be done as below:

$$
R_{d1q1d3q30} = R_{\alpha 1 \beta 1 \alpha 3 \beta 30} e^{j\theta} \tag{7}
$$

Utilizing (7), under healthy conditions the per phase resistances are equal to the resistances in the $d-q$ reference frame ($R_a = R_b = R_c = R_d = R_e = R_e = R_{d1} = R_{q1}$). However, under open phase faults, the resistances in the $d-q$ reference frame become different ($R_{d1} \neq R_{q1}$).

III. STATE SPACE MODELING OF THE FIVE-PHASE SYSTEM UNDER FAULTS

Under different open phase faults, the fault tolerant control algorithm can be established through the state feedback control technique. In general, the state equation of a nonlinear system is presented as follows:

$$
\dot{x} = f(x(t), t, u(t)) \tag{8}
$$

where, $x(t)$ are the states and $u(t)$ are the inputs.

Considering the $d-q$ axes currents are I_d and I_q, which are the states of the five-phase system, $d-q$ axes voltages are V_d and V_q which are the inputs, and the output is as $T_e(t)$, the nonlinear models in (4) and (5) can be written as follows:

$$
\begin{aligned}
\dot{x_1} &= -\frac{1}{L_{d1}} R_{d1} x_1(t) + \frac{1}{L_{q1}} \omega_r (L_{q1} x_2(t) - \lambda_{PM}) + \frac{1}{L_{d1}} u_1(t) \\
\dot{x_2} &= -\frac{1}{L_{q1}} R_{q1} x_2(t) - \frac{1}{L_{q1}} \omega_r (L_{d1} x_1(t)) + \frac{1}{L_{q1}} u_2(t) \\
y(t) &= \frac{5}{4} P[\lambda_{PM} x_1(t) + (L_{d1} - L_{q1}) x_1(t) x_2(t)]
\end{aligned} \tag{9}
$$

where R_{d1} and R_{q1} are the $d-q$ axes resistances (projection of the fundamental).

In this five-phase system, under zero input as $u_1(t) = 0$ and $u_2(t) = 0$, the back electromotive force and the $d-q$ axes current becomes zero, which simplifies that the initial condition are zero as $u_1(t_0) = 0$ and $u_2(t_0) = 0$. Therefore there exists a initial solution as $[x(t)] = 0$. This provides the operating condition as follows:

$$
\begin{aligned}
\hat{u(t)} &= [0] \\
\phi^T &= \begin{bmatrix} [0 & 0] \end{bmatrix}
\end{aligned} \tag{10}
$$

where, $\hat{u(t)}$ and ϕ^T are the initial value of the input and the states, respectively. Equation (10) will be utilized to find the $u_1(t_0) = 0$, $\delta u(t)$ and $\delta x(t)$.

$$
\begin{aligned}
\delta u(t) &= u(t) - \hat{u(t)} = \begin{bmatrix} u_1(t) \\ u_2(t) \end{bmatrix} \\
\delta x(t) &= x(t) - \hat{\phi(t)} = \begin{bmatrix} x_1(t) \\ x_2(t) \end{bmatrix} \\
\dot{\delta x(t)} &= A_x(t) \delta x(t) + B_x(t) \delta u(t)
\end{aligned} \tag{11}
$$

where, $\delta u(t)$ and $\dot{\delta x(t)}$ are the small changes in the inputs and states, respectively, $\dot{\delta x(t)}$ is the derivative of the small change in the states, A_x,B_x, and C_x are the system matrices. These matrices can be derived as follows:

$$
A_x = \begin{bmatrix} \frac{\delta f_1}{\delta x_1} & \frac{\delta f_1}{\delta x_2} \\ \frac{\delta f_2}{\delta x_1} & \frac{\delta f_2}{\delta x_2} \end{bmatrix} = \begin{bmatrix} -\frac{1}{L_d} R_d & \frac{1}{L_d} \omega_r L_q \\ -\frac{1}{L_q} \omega_r L_d & -\frac{1}{L_q} R_q \end{bmatrix} \tag{12}
$$

$$
B_x = \begin{bmatrix} \frac{\delta f_1}{\delta u_1} & \frac{\delta f_1}{\delta u_2} \\ \frac{\delta f_2}{\delta u_1} & \frac{\delta f_2}{\delta u_2} \end{bmatrix} = \begin{bmatrix} \frac{1}{L_d} & 0 \\ 0 & \frac{1}{L_q} \end{bmatrix} \tag{13}
$$

$$
\begin{aligned}
C_x &= \begin{bmatrix} \frac{\delta y}{\delta x_1} & \frac{\delta y}{\delta x_2} \end{bmatrix} \\
&= \begin{bmatrix} \frac{5}{4} P(\lambda_{PM} + (L_d - L_q) x_2) & \frac{5}{4} P(L_d - L_q) x_1 \end{bmatrix}
\end{aligned} \tag{14}
$$

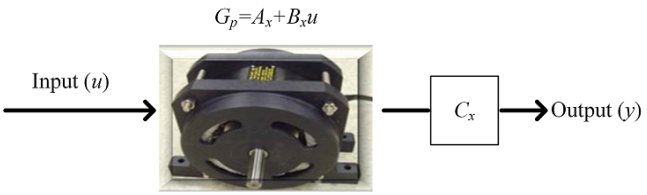

Fig. 3: Open loop system.

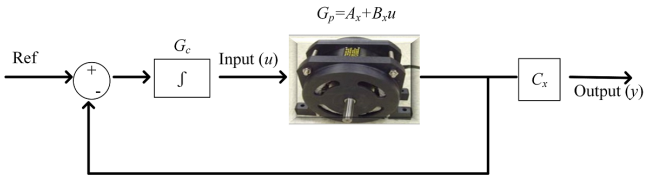

Fig. 4: Closed loop system with an integrator.

IV. PLANT TRANSFER FUNCTION

In this section, the A_x, B_x and C_x are utilized to find the plant transfer functions. As this is a MIMO system, there will be at least two output subsystems from d and q axes components, respectively. Fig. 3 show the simplified block diagram of the open loop system.

A. General Transfer Function of the F-PMa-SynRM

If the system matrices (A_x, B_x, C_x) are known, mathematically the open loop transfer function of any system can be derived as follows:

$$H(s) = C_x(sI - A_x)^{-1}B_x \tag{15}$$

Utilizing (12), (13), (14), and (15), the open loop transfer function of the $d-q$ axes subsystems can be derived as follows:

$$H(s)_{d,OL} = -\frac{5I_dL_d^2\omega(L_d-L_q)-5L_dP(\lambda_{PM}+I_q(L_d-L_q))(R_q+L_qs))}{\sigma_1 L_d} \tag{16}$$

$$H(s)_{q,OL} = \frac{5I_dL_q(L_d-L_q)(R_d+L_dS)+5L_qP\omega L_q(\lambda_{PM}+I_q(L_d-L_q))}{\sigma_1 L_q} \tag{17}$$

where, $\sigma = 4(R_dR_q+L_dR_qS+L_qR_ds+L_d\omega^2L_q+L_dL_qs^2)$.

The open loop transfer functions can be utilized to observe the system present transient performances. Based on the performance requirement, a closed loop system can be designed with an integrator to reduce the system error as in Fig. 4. The closed-loop transfer function of Fig. 4 can be derived as follows:

$$H(s)_{CL} = \frac{G_cG_p}{1+G_cG_p} \tag{18}$$

B. Transfer Function of the F-PMa-SynRM under SPF Condition

The transfer functions of the $d-q$ subsystems in (16) and (17) can be further computed with the machine parameters of the F-PMa-SynRM. The specification of the F-PMa-SynRM is given in Tab I.

TABLE I: Specification of the PMa-SynRM

Parameters	Values
Number of slot/poles	15/4
Rated current (rms)(A)	15.17
Rated voltage (rms) (V)	67
Power (kW)	3
Rated speed (rpm)	1800
Rated Torque (Nm)	15
Phases	5
Phase resistance (R_a)	0.3 Ω
d-axis inductance (L_d)	4 mH
q-axis inductance (L_q)	1 mH
Phase advance	$pi/3$
Nominal d-axis current	Rated current $\times \cos(\pi/3)$
Nominal q-axis current	Rated current $\times \sin(\pi/3)$

Under SPF in phase A ($R_a = 0$), utilizing parameter information in Tab I, the d and q axis resistances become as $R_{d1} = 0.18\Omega$ and $R_{q1} = 0.30\Omega$. Utilizing these R_{d1}, R_{q1}, (16) and (17) become as follows:

$$H(s)_{d,OL,SPF} = \frac{61.18s+7910}{s^2+345s+49030} \tag{19}$$

$$H(s)_{q,OL,SPF} = \frac{57s+14300}{s^2+345s+49030} \tag{20}$$

Using 18, the closed loop transfer of the $d-q$ subsystems under SPF can be derived as follows:

$$H(s)_{d,CL,SPF} = \frac{621.8s+79100}{s^3+345s^2+49700s+79100} \tag{21}$$

$$H(s)_{q,CL,SPF} = \frac{855s+214300}{s^3+345s^2+49890s+210000} \tag{22}$$

Equations (21) and (22) define the system performances providing transient parameters under SPF. These transient parameters are further utilized to design the state feedback gains.

C. Transfer Function of the F-PMa-SynRM under TPAF Condition

Under TPAF in phase A and B ($R_a = R_b = 0$), utilizing parameter information in Tab I, the d and q axis resistances become as $R_{d1} = 0.17\Omega$ and $R_{q1} = 0.19\Omega$. Utilizing these R_{d1}, R_{q1}, the open loop transfer function of the $d-q$ axes subsystems under TPAF are found as below:

$$H(s)_{d,OL,TPAF} = \frac{156.2s+451.5}{s^2+233.6s+32740} \tag{23}$$

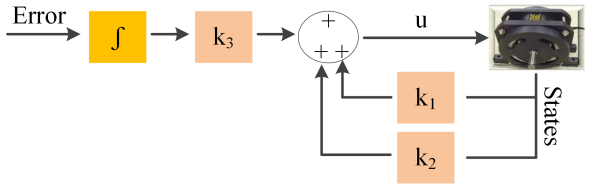

Fig. 5: Simplified state feedback control block diagram.

$$H(s)_{q,OL,TPAF} = \frac{187.5s + 32430}{s^2 + 233.6s + 32740} \tag{24}$$

Similarly the closed loop transfer of the $d-q$ subsystems under TPAF can be derived as follows:

$$H(s)_{d,OL,TPAF} = \frac{156.2s + 451.5}{S^3 + 233.6s^2 + 32900s + 451.5} \tag{25}$$

$$H(s)_{q,OL,TPAF} = \frac{187.5s + 32430}{s^3 + 233.6s^2 + 32930s + 32400} \tag{26}$$

Equations (25) and (26) define the system performances providing transient parameters under TPAF. These transient parameters are further utilized to design the state feedback gains.

V. Designing State Feedback under Open Phase Faults

To design the state feedback gains, (21), (22),(25), (26) are utilized to calculate the eigenvalues under SPF and TPAF. The eigenvalues are the desired pole locations of the system under various operating conditions. Under SPF and TPAF condition the eigenvalues are calculated as follows:

$$\begin{aligned} \zeta_{SPF,1} &= -171.7 + 139i, \\ \zeta_{SPF,2} &= -171.7 - 139i, \\ \zeta_{SPF,3} &= -0.77 - 0.0i \end{aligned}$$

$$\begin{aligned} \zeta_{TPAF,1} &= -116.79 + 138.75i, \\ \zeta_{TPAF,2} &= -116.79 - 138.75i, \\ \zeta_{TPAF,d3} &= -0.99 - 0.0i \end{aligned} \tag{27}$$

These eigenvalues are utilized to develop the state feedback controller by employing the Lyapunov function. For this purpose, the original system matrices A_x, B_x are needed to modify. As there is additional integrator in the control loop, these matrices become as follows:

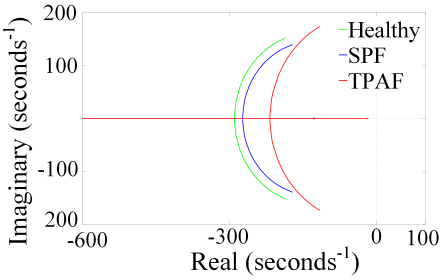

Fig. 6: Root locus of the d-axis system (open loop).

$$\begin{aligned} \tilde{A_x} &= \begin{bmatrix} A_x & 0 \\ -C_x & 0 \end{bmatrix} \\ \tilde{B_x} &= \begin{bmatrix} B_x \\ 0 \end{bmatrix} \end{aligned} \tag{28}$$

For stability criterion, the Lyapunov function can be derived as follows:

$$\tilde{A_x}T - TF = -\tilde{B_x}\tilde{k} \tag{29}$$

where F is an arbitrary square matrix, T is the non-singular matrix, $\tilde{k}$ is the modified matrix which is related to the desired feedback matrix as $k = \tilde{k}T$. By solving (29), the state feedback gains (k) are calculated. In this analysis, the state feedback gains are computed for SPF and TPAF conditions and given as below,

$$\tilde{k}_{SPF} = 10^{-4} \begin{bmatrix} -16.6 + .5i & 2.4 - 1.7i & -5234 + 3i \\ -1.9 - 7i & -4 - 0.13i & -8410 - 12i \end{bmatrix} \tag{30}$$

$$\tilde{k}_{TPAF} = 10^{-4} \begin{bmatrix} -6.6 + 11i & .48 - .2i & -6229 + 24i \\ -7 - 11.2i & -8.14 - 3i & -9943 - 19i \end{bmatrix} \tag{31}$$

VI. Simulation Results

In this section, the Matlab simulation is done to observe the system stability and transient responses. Especially, analyzing the root locus provides information about the system stability. Fig. 6 shows the open loop root locus of the d-axis subsystem under different fault conditions. The locus moves towards the zero axes as the system becomes healthy to single phase open faulty. Under two-phase adjacent fault condition the root locus moves further to the right. In summary, Fig. 6 suggests that under TPAF the systems have less stability margin.

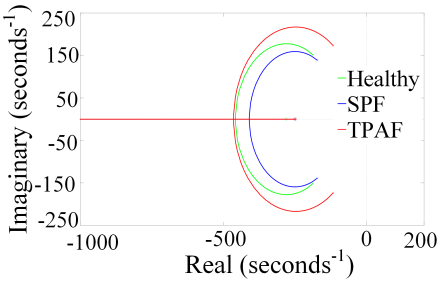

Fig. 7: Root locus of the q-axis system (open loop).

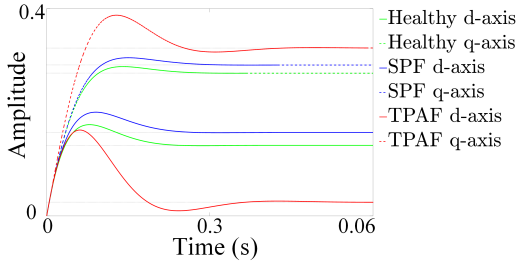

Fig. 8: Step responses of the $d-q$ axes systems (open loop).

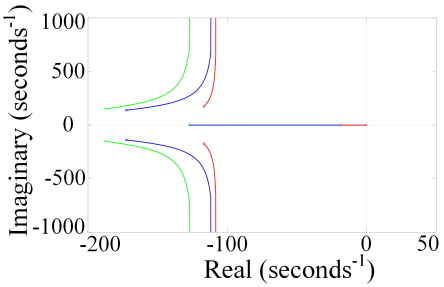

Fig. 9: Root locus of the d-axis system with state feedback.

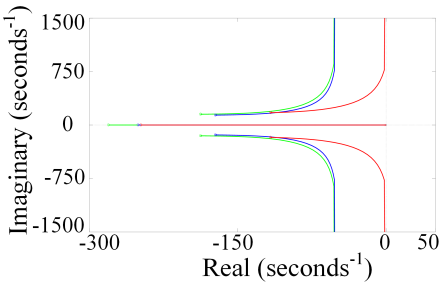

Fig. 10: Root locus of the q-axis system with state feedback.

Fig. 7 shows the open loop root locus of the q-axis subsystem under different fault conditions. In this condition, the locus do not follow any pattern as seen in d-axis case. Under single-phase open fault, the root locus moves towards the right which denotes less system stability under this conditions. However, Fig. 7 suggests that under TPAF the systems have higher overshoot and oscillatory term.

Step responses provide the system performances. Fig. 8 shows the step responses of the open loop system of the d-axis and q-axis subsystems under different fault conditions. Under the healthy condition, the d-axis contains 29.4% overshoot, and q-axis contains 4.7% overshoot. Under single-phase, open fault condition, the overshoot of d-axis and q-axis becomes as 24.2% and 4.8%. Under TPAF condition, the overshoot of d-axis and q-axis becomes as 528.78% and 19.44%. It observed that under TPAF the overshoot becomes quite large. Also, under a two-phase adjacent open fault condition, the time to reach the steady state condition is almost twice than the other conditions meaning the system becomes slow under this situation.

Fig. 9 shows the root locus of the d-axis subsystem under different fault conditions with state feedback. In this situation, initially, a pole in origin is added to reduce the system overshoot. By doing so, it is observed that the locus moves towards the zero axis when a two-phase adjacent open fault occurs. However, unlike the open loop system, the locus ends towards infinity that ensures the system's stability.

Fig. 10 shows the root locus of the q-axis subsystem under different fault conditions with state feedback. Similarly, initially, a pole in origin is added to reduce the system overshoot. It is found, the locus moves towards the zero axes while the system becomes healthy to single-phase fault condition. Under a two-phase adjacent open fault condition, the root locus moves further to the right. However, due to the presence of a pole in origin, unlike the open loop system, the locus ends towards infinity that ensures the system's stability. It is also observed that under TPAF, the system stability is much sensitive to external disturbances as the locus is more closure to zero axes.

Fig. 11 shows the step responses of the closed-loop system of the d-axis and q-axis subsystems under different fault conditions. It is observed there is no overshoot in any fault conditions which was preliminary assumed from the root locus method. However, the system becomes slower with this method compared with the open loop system. The rise time for healthy and SPF condition is close 3.5s. Under TPAF the rise time is around 7s.

VII. Conclusion

In this study, the state space modeling of a five-phase permanent magnet assisted synchronous reluctance motor has been established under different open phase faults. The state space model has been utilized to observe and evaluate the open loop transient performances. To improve the system performances, a closed loop system is developed for the desired system requirements. The performances parameters are utilized to develop the state feed feedback controller by using the Lyapunov function. Detail theoretical analysis has been done for the system considering healthy condition, single phase open fault and adjacent phase open fault conditions. The proposed method provides improved dynamic performances

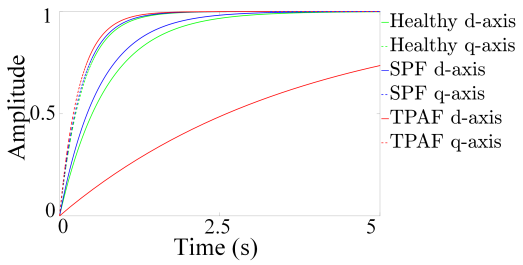

Fig. 11: Step responses of the $d-q$ axes with state feedback.

with the state feedback controller. This control technique can be a promising alternative to the classical method in the industries.

REFERENCES

[1] A. K. M. Arafat and S. Choi, "Fault tolerant control of five-phase permanent magnet assisted synchronous reluctance motor based on dynamic current phase advance," in *2015 IEEE Energy Conversion Congress and Exposition (ECCE)*, Sept 2015, pp. 1208–1214.

[2] A. Arafat and S. Choi, "Optimal phase advance under fault tolerant control of five-phase permanent magnet assisted synchronous reluctance motor," *IEEE Transactions on Industrial Electronics*, vol. PP, no. 99, pp. 1–1, 2017.

[3] S. S. R. Bonthu, A. Arafat, and S. Choi, "Comparisons of rare-earth and rare-earth-free external rotor permanent magnet assisted synchronous reluctance motors," *IEEE Transactions on Industrial Electronics*, vol. 64, no. 12, pp. 9729–9738, Dec 2017.

[4] H. Zhou, W. Zhao, G. Liu, R. Cheng, and Y. Xie, "Remedial field-oriented control of five-phase fault-tolerant permanent-magnet motor by using reduced-order transformation matrices," *IEEE Transactions on Industrial Electronics*, vol. 64, no. 1, pp. 169–178, Jan 2017.

[5] H. Xu, H. A. Toliyat, and L. J. Petersen, "Resilient current control of five-phase induction motor under asymmetrical fault conditions," in *APEC. Seventeenth Annual IEEE Applied Power Electronics Conference and Exposition (Cat. No.02CH37335)*, vol. 1, 2002, pp. 64–71 vol.1.

[6] H. Zhou, W. Zhao, G. Liu, R. Cheng, and Y. Xie, "Remedial field-oriented control of five-phase fault-tolerant permanent-magnet motor by using reduced-order transformation matrices," *IEEE Transactions on Industrial Electronics*, vol. 64, no. 1, pp. 169–178, Jan 2017.

[7] A. Tani, M. Mengoni, L. Zarri, G. Serra, and D. Casadei, "Control of multiphase induction motors with an odd number of phases under open-circuit phase faults," *IEEE Transactions on Power Electronics*, vol. 27, no. 2, pp. 565–577, Feb 2012.

[8] Y. Zhang, T. Chai, and H. Wang, "A nonlinear control method based on anfis and multiple models for a class of siso nonlinear systems and its application," *IEEE Transactions on Neural Networks*, vol. 22, no. 11, pp. 1783–1795, Nov 2011.

[9] M. A. Khanesar, O. Kaynak, and M. Teshnehlab, "Direct model reference takagi-sugeno fuzzy control of siso nonlinear systems," *IEEE Transactions on Fuzzy Systems*, vol. 19, no. 5, pp. 914–924, Oct 2011.

[10] Y. I. Son, I. H. Kim, D. S. Choi, and H. Shim, "Robust cascade control of electric motor drives using dual reduced-order pi observer," *IEEE Transactions on Industrial Electronics*, vol. 62, no. 6, pp. 3672–3682, June 2015.

[11] C. S. Lim, E. Levi, M. Jones, N. A. Rahim, and W. P. Hew, "Fcs-mpc-based current control of a five-phase induction motor and its comparison with pi-pwm control," *IEEE Transactions on Industrial Electronics*, vol. 61, no. 1, pp. 149–163, Jan 2014.

[12] S. S. Ge and Z. Li, "Robust adaptive control for a class of mimo nonlinear systems by state and output feedback," *IEEE Transactions on Automatic Control*, vol. 59, no. 6, pp. 1624–1629, June 2014.

[13] L. Long and J. Zhao, "Switched-observer-based adaptive neural control of mimo switched nonlinear systems with unknown control gains," *IEEE Transactions on Neural Networks and Learning Systems*, vol. 28, no. 7, pp. 1696–1709, July 2017.

[14] M. Pucci, "State space-vector model of linear induction motors," *IEEE Transactions on Industry Applications*, vol. 50, no. 1, pp. 195–207, Jan 2014.

[15] O. Kiselychnyk, M. Bodson, and J. Wang, "Linearized state-space model of a self-excited induction generator suitable for the design of voltage controllers," *IEEE Transactions on Energy Conversion*, vol. 30, no. 4, pp. 1310–1320, Dec 2015.

[16] C. S. Lim, N. A. Rahim, W. P. Hew, and E. Levi, "Model predictive control of a two-motor drive with five-leg-inverter supply," *IEEE Transactions on Industrial Electronics*, vol. 60, no. 1, pp. 54–65, Jan 2013.

[17] M. Rashed, K. B. Goh, M. W. Dunnigan, P. F. A. MacConnell, A. F. Stronach, and B. W. Williams, "Sensorless second-order sliding-mode speed control of a voltage-fed induction-motor drive using nonlinear state feedback," *IEE Proceedings - Electric Power Applications*, vol. 152, no. 5, pp. 1127–1136, Sept 2005.